厚生労働省科学研究補助金
（医療機器開発推進研究事業（活動領域拡張医療機器開発研究事業））
平成２２年度分担研究報告書

慢性心不全の予後を改善するための非侵襲で安全・安心な無痛性 ICD の実用化臨床試験
不整脈高速検出アルゴリズムの実装

分担研究者　吉澤　誠（東北大学 サイバーサイエンスセンター 教授）

研究要旨：
本研究では、著者らが先に提案した、複数の心内心電図信号から得られる指標を用いて算出した重回帰モデルによる致死性不整脈検出アルゴリズムに関して、マイクロコントローラへの実装化の検討を行なった。5 匹のイヌを用いた不整脈誘発実験から得られた洞調律（SR）、上室性不整脈（SVT）、心室頻拍（VT）、および心室細動（VF）のデータに対して、マイクロコントローラ用に高速演算が可能でメモリ消費が少なくなるようアルゴリズムを変更して適用したところ、平均 ROCA は 0.98 以上であった。これは、アルゴリズム変更前の 0.95 と比較して、検出性能を低下させることはないことが確認された。さらに、ICD への実装を想定したマイクロコントローラ上で、提案アルゴリズムを約 56 ms の計算時間と 1 Kbytes 以下のメモリ消費量によって実現できることが示された。ただし、VT、VF の検出に関する偽陰性率が 0.63 であり、さらなるアルゴリズムの改良の余地がある。

A. 研究目的

従来の植込み型除細動器（ICD）は、主として心電図の間隔情報に基づいて不整脈の検出を行なっているため、心室細動（VF）と心室頻拍（VT）を確実に区別することは容易ではない [1-4]。また、付加的情報として心室容積を利用する方法も提案されているが、個人差や呼吸性変動の問題が解決されていない[5-7]。

これらに対して著者らの研究グループでは、複数の心内心電図信号から 2 次元統計量などの 14 個の指標を求め、それらを説明変数とし、不整脈の種類を目的変数とする重回帰モデルを用いる方法を提案してきた[8]。PC 上における提案アルゴリズムの妥当性の検証では、高精度かつ早期の不整脈検出が可能であることが示された。一方、ICD への実装を考慮すると、計算に要するメモリの低減と計算の高速化を図る必要があった。

そこで平成 22 年度では、マイクロコントローラ（以下マイコンと略す）を用いて、ICD への実装化を考慮した不整脈検出アルゴリズムの有用性の検証を行なった。

B. 研究方法

B-1. 実験データ

本研究では、5 頭の成犬を対象とした急性実験を行ない、*in vivo* にてデータを取得した。200 Hz または 1000 Hz のサンプリング周波数で、左心室内、右心室内、および右心房内における心内心電図（Intracardiac electrocardiogram: IECG）を記録した。記録後、すべての心電図に対し、250 Hz にて再サンプリングを行なった。なお、不整脈の自然発生を計測するのは困難なため、人為的な方法によって SVT、VT および VF を模擬した。

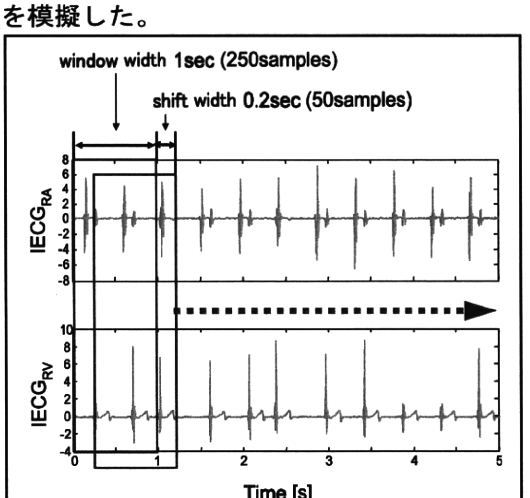

Fig.1 Data acquisition using an 1s long window shifting every 0.2s

最初に，取得した心内心電図データに対して、0.8 Hz～40 Hz の帯域通過型フィルタを用いてノイズ成分を除去した。フィルタ処理後、Fig.1 に示すように、1 s の長さの窓を用いて 0.2 s ずつシフトさせながらデータを抽出した。そし

て、ごとに心内心電図の特徴量に基づく指標を算出した。

なお、C 上での処理は、値解析ソフトウェア MATLAB R2006b（MathWorks 社）を用いて行なった。

B-2. 重回帰モデルを用いた不整脈の分類法

本研究では、4 種類の心調律の状態 SR、SVT、VT、および VF の鑑別を行うために、次のような、心内心電図の特徴量に基づく複数の指標を入力とした重回帰モデルに基づく方法を用いた。

いま、上述のデータ窓の 0.2 s のシフト毎に増える離散時間を k とする。各データに対して全部で m 個の指標を求め、これらを要素とする $m \times 1$ ベクトルを $\boldsymbol{x}(k)$とおく。また、4 種類の心調律の種類 SR、SVT、VT、および VF に対応する番号をそれぞれ $i = 1,\cdots,4$ とするとき、検出結果を

$$y_i(k) = \begin{cases} 1 & (i\text{番目の心調律に該当}) \\ 0 & (i\text{番目の心調律に該当せず}) \end{cases} \qquad (1)$$

で表す。$y_i(k)$を要素とする 4×1 ベクトル $\boldsymbol{y}(k) = [y_1(k),...,y_4(k)]^{\mathrm{T}}$ を検出結果ベクトルと呼ぶ。

データベクトル $\boldsymbol{x}(k)$を説明変数とし、検出結果ベクトル $\boldsymbol{y}(k)$を目的変数とする重回帰モデルを

$$\boldsymbol{y}(k) = \boldsymbol{A}\boldsymbol{x}(k) + \boldsymbol{e}(k) \qquad (2)$$

で表す。ここで、$\boldsymbol{A}$ は $4 \times m$ 行列であり、4×1 ベクトル $\boldsymbol{e}(k)$は残差である。

本研究では、先行研究[8]の結果を踏まえて、指標の数を後述のように $m = 14$ とし、最小 2 乗法により(2)式の重回帰モデルの係数行列 $\boldsymbol{A}$ を計算した。

運用時には、逐次的に計算した各指標から作られる $\boldsymbol{x}(k)$を，(2)式で $\boldsymbol{e}(k) = 0$ としたモデルに入力し、SR、SVT、VT、および VF に対応する 4 つの目的変数 $y_i(k)$の推定値を計算し、それらの中の最大値に対応する不整脈番号をその時の不整脈の種類として判定する。

B-3. 心内心電図から得られる指標

本研究では、4 種類の心調律の状態 SR、SVT、VT、および VF の鑑別を行うために、次のような、心内心電図の特徴量に基づく複数の指標を入力とした重回帰モデルに基づく方法を用いた。本研究では、重回帰モデルの入力として、以下に示す 14 個の特徴量を用いた。

1) ヒストグラムに基づく指標 (Histogram)

SR、SVT、および VT のように心房から心室への 1:1 伝導が保持される場合は、心房と心室での心電図信号の独立性は低く、VF 時は独立性が高くなると考えられる。本研究では、2 種類の心電図に対して、Fig. 2 のように 5 個 × 5 個のビンで表される 2 次元のヒストグラムである同時度数分布を求め、さらにそこから 2 つの信号の独立性を判定するために、Pearson の χ^2 統計量を計算した。また、2 つの心電図信号の不規則性を標準偏差σで評価した。

本研究では左心室心電図 $IECG_{\mathrm{LV}}$ と右心室心電図 $IECG_{\mathrm{RV}}$ の間、および右心房心電図 $IECG_{\mathrm{RA}}$ と右心室心電図 $IECG_{\mathrm{RV}}$ の間に対して、それぞれ χ^2 統計量およびσを求めた。

2) 心周期に基づく指標 (Period)

心電図から得られる基本的な指標として心周期の算出を行なった。従来法では、心電図にノイズが多く含まれた場合でも R 波が検出できるように自己相関関数から算出する方法を用いていたが、本研究では計算量を考慮して、心電図信号の一次微分の値を用いて R 波を検出し、心周期を求めた。

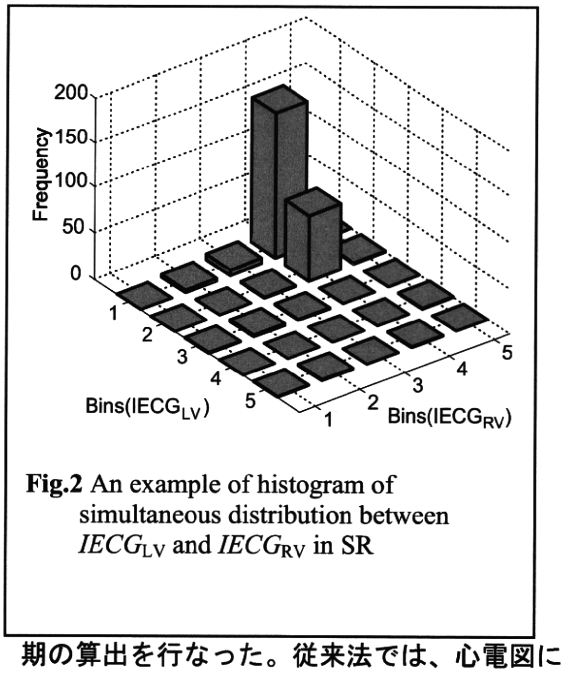

Fig.2 An example of histogram of simultaneous distribution between $IECG_{\mathrm{LV}}$ and $IECG_{\mathrm{RV}}$ in SR

本研究では、$IECG_{\mathrm{LV}}$, $IECG_{\mathrm{RV}}$ および $IECG_{\mathrm{RA}}$ からそれぞれの心周期 $Period_{\mathrm{LV}}$, $Period_{\mathrm{RV}}$ および $Period_{\mathrm{RA}}$ を算出した。さらに、$Period_{\mathrm{RV}}$ とそれ以外の心周期との比として $Period_{\mathrm{LV}}$ / $Period_{\mathrm{RV}}$ と $Period_{\mathrm{RA}}$ / $Period_{\mathrm{RV}}$ を算出した。

3) 相対的遅れ時間による指標 (Delay)

2 つの心電図における相対的な遅れ時間を指標として算出した。従来法では、2 つの心電図間の相互相関関数を用いて算出していたが、計算量を考慮し、Period の算出時に得られる R 波の情報を用いて算出した。

本研究では、$IECG_{\mathrm{RV}}$ を基準信号とし、$IECG_{\mathrm{RA}}$

から $IECG_{RV}$ までの遅れ時間および $IECG_{RV}$ から $IECG_{LV}$ までの遅れ時間を指標として用いた。

4) IECG による複素数平面から得られる指標 (Complex)

最後に、2 つの心電図をそれぞれ実部と虚部とする複素数と見なし、その偏角と絶対値から指標を求める。

複素数 Z を

$$Z = IECG_{RV} + i \cdot IECG_{LV} \qquad (3)$$

と定義する。ここで i は虚数単位である。

Z の偏角のうち、第一象限に含まれるものの平均値と第三象限に含まれるものの平均値をそれぞれ指標として求めた。また、脱分極の長さを

$$|Z| > 0.05 \cdot \max_{\text{心周期内}} |Z| \qquad (4)$$

となるサンプル点の個数で近似し、指標とした。

なお、偏角の算出に必要な逆正接 (arctan) 演算については、計算時間の短縮のために、ライブラリ関数を用いずにルックアップテーブルを用いて行なった。

B-4. 評価方法

提案手法の有用性を評価するために、W= 5221 個の全データセットから、無作為に K = 400 個の窓で区切られたトレーニングデータを選択し、残りの W − K = 4821 個のデータはテストデータとして心調律の分類を行なった。さらに、提案方法のロバスト性を評価するため、この操作を 100 回繰り返し行なった。

トレーニングデータによって得られた重回帰モデルの分類性能の評価を行なうため、テストデータの分類結果におけるそれぞれの心調律の感度と特異度を算出し、ROC(receiver operating characteristic)曲線における曲線下の面積 ROCA(area under the ROC)を算出した。ROCA はその値が 1 に近いほど、分類器としての有効性が高いといえる評価基準である。ROC 曲線のグラフは、2 値分類システムにおいて、縦軸が感度(*Sensitivity*)、横軸が 1 − 特異度(*Specificity*)で表される。*Sensitivity* と *Specificity* はそれぞれ

$$Sensitivity = \frac{TP}{TP + FN} \qquad (5)$$

$$Specificity = \frac{TN}{TN + FP} \qquad (6)$$

のように定義される。ここで、*TP* は true positive (真陽性) のデータの個数、*FN* は false negative (偽陰性) のデータの個数、*TN* は true negative (真陰性) のデータの個数、*FP* は false positive (偽陽性) のデータの個数を表す。

本研究では、先行研究[8]のアルゴリズムと指標の計算方法を変更した提案アルゴリズムの比較を行なった。

(倫理面への配慮)

実験に用いたイヌは、国立循環器病研究センター研究所の倫理委員会の規定に従って適切に管理され、実験は苦痛を与えない麻酔下で行われた。

B-5. ICD へのアルゴリズムの実装化

提案手法の妥当性を評価するために、全データセットから、提案アルゴリズムの ICD への実装化について、計算時間およびメモリ消費量の面から有用性を検証する。

ICD に実装するアルゴリズムについて、計算時間とメモリ消費量を考慮し、次のような構成とした。重回帰モデルの推定には多くの計算時間が必要であるため、PC 上で MATLAB を用いてモデル推定を行なうものとした。実用上は、PC を用いて推定した重回帰モデルの係数をもとに、ICD 上で心調律の分類を行なえばよい。そして、心内心電図から 14 個の指標を計算する部分および重回帰モデルの係数を用いて心調律の分類を行なう部分を、ICD に実装することとした。

ICD への実装を検証するために、低消費電力で動作するマイクロコントローラとして MSP430 (テキサス・インスツルメンツ社) を用いた。また、開発環境として、Code Composer Essentials v3.1 (テキサス・インスツルメンツ社) を使用し、C 言語によるアルゴリズムの実装を行なった。計算時間ならびにメモリ消費量に関しては、Code Composer Essentials のデバッガの機能を用いることで検証を行なった。

実装用に求められる仕様として、動作周波数 12MHz のもとで、計算時間は 1 つの窓から次の窓までのシフト時間である 0.2s をもとに、その半分の時間である 0.1s 以下とした。また、メモリ消費量は RAM 領域において心電図データのバッファとしての 768 bytes を含む条件の下で 1 Kbytes 以下とした。

C. 結　果

先行研究[8]のアルゴリズムを用いて分類を行なった場合と提案方法を用いて分類を行なった場合の、ROCA による評価の比較結果を Fig.3 に示す。

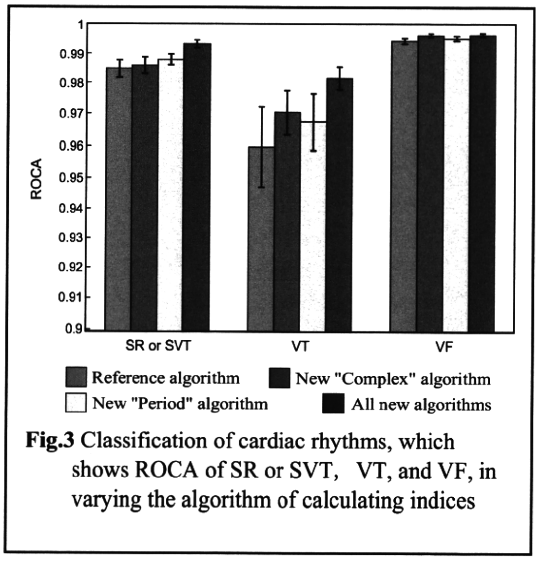

Fig.3 Classification of cardiac rhythms, which shows ROCA of SR or SVT, VT, and VF, in varying the algorithm of calculating indices

図中では、先行研究のアルゴリズムを Reference algorithm、Reference algorithm から Period と Delay の算出方法を変更したものを New "Period" algorithm , Reference algorithm から Complex の算出方法を変更したものを New "Complex" algorithm、すべて新しいアルゴリズムに変更したものを All new algorithms として示した。ただし，4 つの心調律への分類のうち、SR と SVT についてはいずれの場合でも ICD が作動しないため同じカテゴリーとして分類した。

次に、提案アルゴリズムを MSP430 に搭載し、1 つの窓におけるそれぞれの指標の計算時間は Table 1 のようになった。また、メモリ消費量は Table 2 のようになった。全指標の計算時間は約 56 ms、メモリ消費量は 1.02M bytes であった。

Table 1 Computational time of calculating indices

Index	Histogram	Period	Delay	Complex
Computational time [ms]	18	5	< 1	32

Table 2 Memory usage of the proposed algorithm in MSP430

Section	IECG buffer	Indices	Stack	Others
Memory [bytes]	768	56	160	32

D. 考　察

D-1. 提案したアルゴリズムの評価

Fig.3 より、先行研究のアルゴリズムに比べて、ICD への実装化を考慮に入れた提案方法のアルゴリズムのほうが、検出性能が高く、0.98 以上の検出性能が得られた。特に、心周期（Period）と遅れ（Delay）を算出するアルゴリズムについて、相関関数を用いた従来法では 100 ms 以内という計算時間の仕様を満たすことが困難であることが確認されており、心電図の一次微分の値を用いて R 波を検出する方法のほうが有用であると考えられる。ただし、心電図の計測環境によっては、ノイズ対策が必要となる可能性があるので、今後検討する必要がある。複素数平面から得られる指標に関しては、arctan 演算のテーブル化による検出性能の低下は見られず、高速化を実現しながら性能が維持できたと言える。

計算時間およびメモリ消費量に関しては、Table 1 および Table 2 より、求められる仕様を満たしていることがわかる。特に、計算時間は約 56 ms と要求の約 1/2 であり、今後のアルゴリズムの改良に伴う計算量の変化に対し、柔軟に対応できると考えられる。一方、メモリ消費量に関しては、仕様に対して余裕が少ないため、さらに省メモリ化を図る必要があると考えられる。

以上のように提案アルゴリズムの ICD への実装は、計算時間やメモリ消費量の観点から可能であると考えられるが、ヒトを対象とした実用面では次のような問題点を抱えている。

まず、計測できる心内心電図のチャンネル数に制限がある場合、例えば、本研究では 3ch のデータを用いているがデバイスの仕様等で 2ch のデータしか得られない場合、重回帰モデル推定用の指標をすべて計算することはできない。先行研究[8]によると、指標の個数を 14 個から減少させると、約 1～10%程度 ROCA の値が低下することがわかっている。それゆえ、検出性能を保つためにアルゴリズムの変更が必要となると考えられる。

また、ヒトの心電図に対する有効性を検証する場合、ROCA の値だけではなく VT、VF の検出における偽陰性率が重要となる。しかし、提案アルゴリズムでは偽陰性率が 0.63 であり、これをさらに向上させる必要がある。

E. 結　論

本研究では、心内心電図から得られる複数の指標を用いた重回帰モデルを用いて 4 つの心調律(SR、SVT、VT、VF)に分類する方法において、従来法のアルゴリズムから高速でメモリ消費量の少ないアルゴリズムへと変更を行なっても、検出性能を低下させることないことが確認された。さらに、ICD への実装を想定したマイクロコントローラ上でも、提案アルゴリズムを約 56 ms の計算時間と 1 Kbytes 以下のメモリ消費量によって実現できることが示された。

今後は、イヌの心電図だけではなく、ヒトの

心電図に対する有効性の検証も重要である。
そのうえで、VT、VF の検出における偽陰性率がまだ実用化に耐え得る値ではないため、今後はさらなるアルゴリズムの改良が必要であると考えられる。

参考文献

1. Eberhardt F, Peters W, Bode F, et al.: Wave Undersensing Caused by an Algorithm Intended to Enhance Sensing Specifity in an Implantable Cardioverter Defibrillator. PACE, 2003; 26(8): 1776-1777.
2. Aliot E, Nitzsche R, Ripart A: Arrhythmia detection by dual-chamber implantable cardioverter defibrillators. A review of current algorithms, Europace, 2004; 6(4): 273-286.
3. Brugada J, Mont L, Figueiredo M, et al.: Enhanced detection criteria in implantable defibrillators. J Cardiovasc Electrophysiol, 1998; 9, 261-268.
4. Neuzner J, Pitschner HF, Schlepper M: Programmable VT detection enhancements in implantable cardioverter defibrillator therapy. PACE, 1995; 18, 539-547.
5. Kinoshita H, Yoshizawa M, Inagaki M, Uemura K, Sugimachi M, Sunagawa K: Development of an algorithm for early detection of fatal cardiac arrhythmia for implantable cardioverter-defibrillator using a self-organizing map. Proc. of International Symposium on Bio- and Nano-Electronics in Sendai, 2006; 101-102.
6. Kinoshita H, Yoshizawa M, Inagaki M, Uemura K, Sugimachi M, Sunagawa K: Development of an algorithm for detection of fatal arrhythmias for implantable cardioverter-defibrillator using a self-organizing map. Proc. of 28th Annual International conference IEEE Engineering in Medicine and Biology Society, 2006; 4370-4373.
7. Kinoshita H, Yoshizawa M, Inagaki M, Uemura K, Sugimachi M, Sunagawa K: An algorithm for fatal arrhythmia detection in a new implantable cardioverter-defibrillator. Proc. of the Second International Symposium on Bio- and Nano-Electronics in Sendai, 2006; 61-62.
8. 阿部　誠, テルマ ケイコ スガイ, 吉澤　誠, 山家智之, 清水一夫, 後藤　萌, 稲垣正司, 杉町　勝, 砂川賢二：重回帰分析を用いた致死性不整脈検出アルゴリズムに関する検討, 生体医工学, 2010; 48(6): 577-583.

F. 健康危険情報

該当なし.

G. 研究発表

G-1. 論文

1. 阿部　誠, テルマ ケイコ スガイ, 吉澤　誠, 山家智之, 清水一夫, 後藤　萌, 稲垣正司, 杉町　勝, 砂川賢二：重回帰分析を用いた致死性不整脈検出アルゴリズムに関する検討, 生体医工学, 48(6), 577-583, 2010.

G-2. 学会発表

1. 阿部　誠, テルマ ケイコ スガイ, 吉澤　誠, 清水一夫, 後藤　萌, 稲垣正司, 杉町　勝, 砂川賢二：重回帰分析を用いた致死性不整脈検出アルゴリズムに関する検討, 生体医工学シンポジウム2010, CD-ROM, 2010.
2. 阿部　誠, テルマ ケイコ スガイ, 吉澤　誠, 清水一夫, 後藤　萌, 稲垣正司, 杉町　勝, 砂川賢二：重回帰モデルを用いた致死性不整脈検出アルゴリズムとそのICD への実装化, 第11回計測自動制御学会システムインテグレーション部門講演会, 202-205, 2010.
3. Telma Keiko Sugai,Akira Tanaka, Makoto Yoshizawa, Yasuyuki Shiraishi, Atsushi Baba, Tomoyuki Yambe, Shin-ichi Nitta: Influence of Rotary Blood Pumps over Preload Recruitable Stroke Work, 32nd Annual International Conference of the IEEE EMBS, Buenos Aires, Argentina, August 31 - September 4, 2010.

G-3. 新聞報道

なし

H. 知的所有権の取得状況

なし

厚生労働省科学研究補助金
（医療機器開発推進研究事業）
平成２２年度分担研究報告書

慢性心不全の予後を改善するための非侵襲で安全・安心な無痛性 ICD の実用化臨床試験
植込み型突然死防止装置の開発（分担課題名）

分担研究者　清水　一夫（オリンパス株式会社　医療技術開発本部　医療探索部　部長）

研究要旨：
無痛性除細動機能を実現するため、仕様を検討し、装置の開発を行った。　過去開発してきた植込み型突然死防止装置（ICD）本体の構成を見直し、装置の小型化、低消費電力化を実現した。既存機能として VVI, DDD、CRT（両心室再同期療法）等の最新のペースメーカー機能、頻拍治療、除細動治療の各機能は仕様通りであることを確認した。
今年度は植込み型 ICD 装置実現に向け、植込み可能な 100cc サイズを目指し、試作を行い、その性能について評価を実施した。その結果、ほぼ目標の消費電力で動作可能な装置を試作することができた。
また、さらなる小型、低消費電力化に関しては、信号検出用 LSI の開発をすすめていく必要があり、今年度、LSI 化の目処がついたので、来年度、試作検証を行う予定である。

A. 研究目的

植え込み型除細動器の高性能化を図りつつ、使用する患者の負担を軽減するには、小型化と長寿命化が重要である。

既存 ICD の実現に必要な技術を確立した上で、痛くない除細動機能、及び超小型低消費電力化電子回路の実現を目指す。

弊社分担業務として、植え込み可能な ICD 本体の試作機開発、及び ICD 本体を制御する為のプログラマの開発を行い、機能の確認を行うことを目的とする。

B. 研究方法

B-1. 開発手順

昨年度実施した ICD 国際規格に基づく試験結果を受けて、植込み実験可能な ICD 装置として 100cc サイズの装置開発を目指し、試作を行った。

まず、検証に使用した機器の構成をベースに回路構成を検討し、シミュレーションにより、回路動作の検証を実施した。

また、過去５年間、厚生労働省科学研究補助金により、植込み型突然死防止装置の開発（Ｈ１５－フィジー００１）を行ってきた成果に基づき、試作実験機の開発を行った。試作実験機の試験は、心拍を模擬した信号発生器により、試験を行い、この試験にて有効性が確認された後、動物実験を行い性能評価を行った。

＜倫理面への配慮＞

動物実験については、九州大学、国立循環器病センター研究所にご協力を頂き、動物実験に関する指針に準拠して行った。

B-2. 植込み型突然死防止装置の研究

B-2.1 痛くない除細動機能の研究

シミュレータを利用して、電極構造や除細動パターンのシミュレーションを実施し、超低エネルギーで除細動できる電極の構造の見直しを行った。また、試作して実験検証を実施した。

B-2.2 植込み型除細動器の開発

本年度は本体の小型化を行うため、高電圧回路をベアチップ実装し、小型化を図った。また、試作装置を用いて、ICD の性能の評価を実施した。

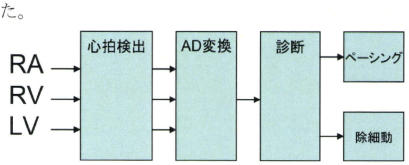

図１　ICD 装置の構成

C. 研究結果

C-1. 痛くない除細動機能の研究

痛くない除細動実現のため、小型 ICD 装置により除細動出力の実験を行ったところ、２相性出力が出せることを確認した。

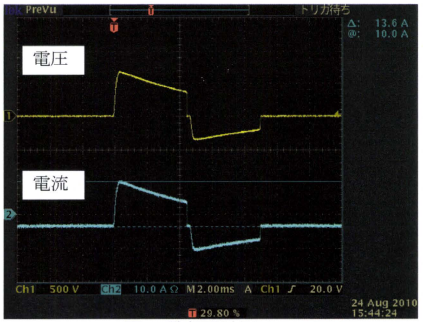

図２　除細動波形

C-２. 植込み型除細動器の開発

①消費電力

心拍検出時の消費電力を測定したところ、122uA

となった。

②心拍検出

ICD 国際規格（EN45502-2-2）における要求仕様に従い試験を実施した。

図３に心拍検出用評価回路を示す。

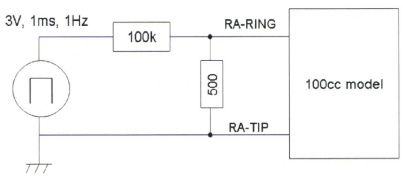

図３　心拍検出評価回路

試験の結果、図４に示すように心拍信号に従い、検出できていることを確認した。

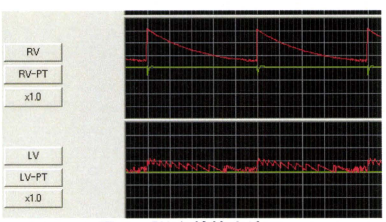

図４　RV 心拍検出波形

③ペーシング出力

負荷抵抗 500Ω にて出力電圧、パルス幅、レートについて測定を行った。その結果、パルス幅、レートについては設定通りの出力になっていることを確認した。出力電圧については誤差が図５のように生じている。

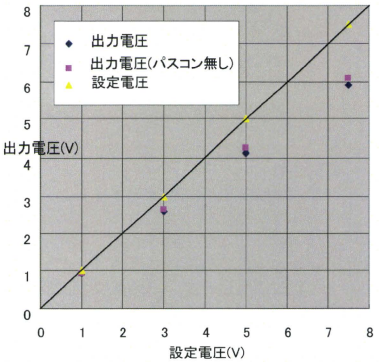

図５　ペーシング出力電圧の測定

④ インピーダンス測定

負荷抵抗 500Ω、1KΩにて測定を行い、±10%以内の測定精度を確認した。

D. 考察

昨年度試作した ICD 装置の構成をさらに見直し、小型化と低消費電力化を実現したが、図４の検出波形のように RV の心拍に対して、ATC の LV 側レベルにノイズが生じている。これは図１の構成の AD 変換器の変換タイミングにより生じていることが確認できた。従って、各心拍信号の AD 変換のタイミングを調整することにより、ノイズを除去した。図６に LV 側に心拍信号を入力した場合でもノイズが出ない例を提示する。

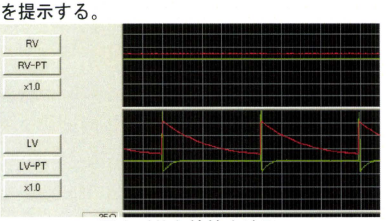

図６　LV 心拍検出波形

AD 変換器の変換タイミングを調整した後、LV 側のノイズが除去された結果を図７に示す。

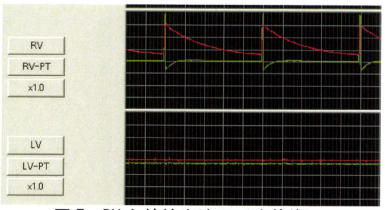

図 7　RV 心拍検出波形（改善後）

次にペーシング出力についてであるが、ペーシング出力電圧を設定する基準電圧の発生回路に不具合があり、設定した電圧レベルが出ていないことが判った。これは基準電圧生成回路の消費電力を削減するため、抵抗値を高く設定したことが原因である。基準電圧を設計通りの値にすれば、ペーシング出力は設定電圧レベルになることを確認した。今後、低消費化を検討する上では常時動作する回路の消費電力をどのように抑えるかがポイントとなる。

今後、さらなる低消費電力化を行うため、上記、基準電圧回路および検出回路の低消費電力化を検討する必要がある。検出回路については現在、アナログ回路で実現しているが、デジタル処理化を行うことにより、さらなる低消費電力化が可能なことが今期の要素検討により、判ってきた。従って、来年度は検出回路のデジタル化実現に向け、開発を進めていく予定である。

E. 結論

本年度は昨年度の試作機をベースに設計の見直しを行い、100cc サイズでの植込み型 ICD 装置の試作機を開発した。
消費電力も大幅に改善することができ、目標とした 100uA に近い、122uA を達成し、昨年度の 1/5 となった。しかし、ICD 装置の植込み期間を考えると 50uA 以下にする必要があり、さらなる小型、低消費電力化が必要である。

アルゴリズムの開発並びに動物実験を行うにあたり、九州大学、国立循環器病研究センター研究所、東京大学、東北大学の関係者の皆様より、多大なるご助言、ご協力をいただきました。
関係者の皆様に心より感謝申し上げます。

F. 健康危険情報

特になし。

G. 研究発表

特になし。

H. 知的所有権の取得状況

特になし。

研究成果の刊行に関する一覧表

書籍

なし

雑誌

1. Hashimoto T, Ichiki T, Ikeda J, Narabayashi E, Matsuura H, Miyazaki R, Inanaga K, Takeda K, Sunagawa K. Inhibition of MDM2 Attenuates Neointimal Hyperplasia via Suppression of Vascular Proliferation and Inflammation. Cardiovasc Res. In press, 2011.

2. Kamiya A, Kawada T, Shimizu S, Sugimachi M. Closed-loop spontaneous baroreflex transfer function is inappropriate for system identification of neural arc but partially appropriate for peripheral arc: a predictability analysis. J Physiol. In press, 2011.

3. Uemura K, Kawada T, Sunagawa K, Sugimachi M. Peak Systolic Mitral Annulus Velocity Reflects the Status of Ventricular-Arterial Coupling-Theoretical and Experimental Analyses. J Am Soc Echocardiogr. In press, 2011.

4. Okada J,Washio T, Maehara A, Momomura S,Sugiura S,Hisada T. Transmural and apicobasal gradients in repolarization contribute to T wave genesis in human surface ECG. Am J Physiol Heart Circ Physiol. In press, 2011.

5. Hirooka Y, Kishi T, Sakai K, Takeshita A, Sunagawa K. Imbalance of central nitric oxide and reactive oxygen species in the regulation of sympathetic activity and neural mechanisms of hypertension. Am J Physiol Regul Integr Comp Physiol. 300: R818-R826, 2011.

6. Chen L, Nakano K, Kimura S, Matoba T, Iwata E, Miyagawa M, Tsujimoto H, Nagaoka K, Kishimoto J, Sunagawa K, Egashira K. Nanoparticle-mediated delivery of pitavastatin into lungs ameliorates the development and induces regression of monocrotaline-induced pulmonary artery hypertension. Hypertension. 57: 343-350, 2011.

7. Fujino T, Nishizaka M, Yufu T, Sunagawa K. A case of multiple focal nodular hyperplasia in the liver which developed after heart transplantation. Intern Med. 50: 43-46, 2011.

8. Kawada T, Shimizu S, Kamiya A, Sata Y, Uemura K, Sugimachi M. Dynamic characteristics of baroreflex neural and peripheral arcs are preserved in spontaneously hypertensive rats. Am J Physiol Regul Integr Comp Physiol. 300: R155-R165, 2011

9. Yamamoto H, Kawada T, Kamiya A, Miyazaki S, Sugimachi M. Involvement of the mechanoreceptors in the sensory mechanisms of manual and electrical acupuncture. Auton Neurosci. 160: 27-31, 2011

10. Mizuno M, Kawada T, Kamiya A, Miyamoto T, Shimizu S, Shishido T, Smith SA, Sugimachi M. Exercise training augments the dynamic heart rate response to vagal but not sympathetic stimulation in rats. Am J Physiol Regul Integr Comp Physiol. 300: R969-R977, 2011

11. Washio T, Hisada T. Convergence Analysis of Inexact LU-type Preconditioners for Indefinite Problems in Incompressible Continuum Analysis. JJIAM 28: 89-117, 2011

12. Kish i T, Sunagawa K. Baroreflex sensitivity might predict responders to milrinone in patients with heart failure. Int Heart J. 51: 411-415, 2010.

13. Sunagawa K, Sugimachi M. Development of artificial bionic baroreflex system. Conf Proc IEEE Eng Med Biol Soc. 2010: 3446-3448, 2010.

14. Sunagawa K. The pressure-volume relationship of the heart: past, present and future. Conf Proc IEEE Eng Med Biol Soc. 2010: 3554-3555, 2010.

15. Sugimachi M, Sunagawa K, Uemura K, Shishido T. Physiological significance of pressure-volume relationship: a load-independent index and a determinant of pump function. Conf Proc IEEE Eng Med Biol Soc. 2010: 3553, 2010.

16. Uemura K, Sugimachi M, Kawada T, Sunagawa K. Automated drug delivery system for the management of hemodynamics and cardiac energetic in acute heart failure. Conf Proc IEEE Eng Med Biol Soc. 2010: 5222-5225, 2010.

17. Sugimachi M, Sunagawa K, Uemura K, Kamiya A, Shimizu S, Inagaki M, Shishido T. Estimated venous return surface and cardiac output curve precisely predicts new hemodynamics after volume change. Conf Proc IEEE Eng Med Biol Soc. 2010: 5205-5208, 2010.

18. Sakamoto T, Murayama Y, Tobushi T, Sakamoto K, Tanaka A, Tsutsumi T, Sunagawa K. How to quantitatively synthesize dynamic changes in arterial pressure from baroreflexly modulated ventricular and arterial properties. Conf Proc IEEE Eng Med Biol Soc. 2010: 2869-2871, 2010.

19. Inanaga K, Ichiki T, Miyazaki R, Takeda K, Hashimoto T, Matsuura H, Sunagawa K. Acetylcholinesterase inhibitors attenuate atherogenesis in apolipoprotein E-knockout mice. Atherosclerosis. 213: 52-58, 2010.

20. Ito K, Hirooka Y, Sunagawa K. Blockade of mineralocorticoid receptors improves salt-induced left-ventricular systolic dysfunction through attenuation of enhanced sympathetic drive in mice with pressure overload. J Hypertens. 28: 1449-1458, 2010.

21. Oda S, Nagahama R, Nakano K, Matoba T, Kubo M, Sunagawa K, Tominaga R, Egashira K. Nanoparticle-mediated endothelial cell-selective delivery of pitavastatin induces functional collateral arteries (therapeutic arteriogenesis) in a rabbit model of chronic hind limb ischemia. J Vasc Surg. 52: 412-420, 2010.

22. Hirooka Y, Sagara Y, Kishi T, Sunagawa K. Oxidative stress and central cardiovascular regulation. - Pathogenesis of hypertension and therapeutic aspects -. Circ J. 74: 827-835, 2010.

23. Kishi T, Hirooka Y, Konno S, Ogawa K, Sunagawa K. Angiotensin II type 1 receptor-activated caspase-3 through ras/mitogen-activated protein kinase/extracellular signal-regulated kinase in the rostral ventrolateral medulla is involved in sympathoexcitation in stroke-prone spontaneously hypertensive rats. Hypertension. 55: 291-297, 2010.

24. Miyashita H, Aizawa A, Hashimoto J, Hirooka Y, Imai Y, Kawano Y, Kohara K, Sunagawa K, Suzuki H, Tabara Y, Takazawa K, Takenaka T, Yasuda H, Shimada K. Cross-sectional characterization of all classes of antihypertensives in terms of central blood pressure in Japanese hypertensive patients. Am J Hypertens. 23: 260-268, 2010.

25. Kishi T, Hirooka Y, Konno S, Sunagawa K. Sympathoinhibition induced by centrally administered atorvastatin is associated with alteration of NAD(P)H and Mn superoxide dismutase activity in rostral ventrolateral medulla of stroke-prone spontaneously hypertensive rats. J Cardiovasc Pharmacol. 55: 184-190, 2010.

26. Takemoto M, Nakashima A, Muneuchi J, Yamamura K, Shiokawa Y, Sunagawa K, Tominaga R. Para-Hisian pacing for a pediatric patient with a congenitally corrected transposition of the great arteries (SLL). Pacing Clin Electrophysiol. 33: e4-e7, 2010.

27. Kamiya A, Kawada T, Mizuno M, Shimizu S, Sugimachi M. Parallel resetting of arterial baroreflex control of renal and cardiac sympathetic nerve activities during upright tilt in rabbits. Am J Physiol Heart Circ Physiol. 298: H1966-H1975, 2011.

28. Kawada T, Li M, Kamiya A, Shimizu S, Uemura K, Yamamoto H, Sugimachi M. Open-loop dynamic and static characteristics of the carotid sinus baroreflex in rats with chronic heart failure after myocardial infarction. J Physiol Sci. 60: 283-298, 2010.

29. Kawada T, Akiyama T, Shimizu S, Kamiya A, Uemura K, Sata Y, Shirai M, Sugimachi M. Large conductance Ca2+-activated K+ channels inhibit vagal acetylcholine release at the rabbit sinoatrial node. Auton Neurosci. 156: 149-151, 2010.

30. Mizuno M, Kawada T, Kamiya A, Miyamoto T, Shimizu S, Shishido T, Smith SA, Sugimachi M. Dynamic characteristics of heart rate control by the autonomic nervous system in rats. Exp Physiol. 95: 919-925, 2010

31. Shimizu S, Shishido T, Une D, Kamiya A, Kawada T, Sano S, Sugimachi M. Right ventricular stiffness constant as a predictor of postoperative hemodynamics in patients with hypoplastic right ventricle: a theoretical analysis. J Physiol Sci. 60: 205-212, 2010

32. Takahama H, Asanuma H, Sanada S, Fujita M, Sasaki H, Wakeno M, Kim J, Asakura M, Takashima S, Minamino T, Komamura K, Sugimachi M, Kitakaze M. A histamine H receptor blocker ameliorates development of heart failure in dogs independently of beta-adrenergic receptor blockade. Basic Res Cardiol. 105: 787-794, 2010

33. Uemura K, Zheng C, Li M, Kawada T, Sugimachi M. Early short-term vagal nerve stimulation attenuates cardiac remodeling after reperfused myocardial infarction. J Card Fail. 16: 689-699, 2010.

34. Une D, Shimizu S, Kamiya A, Kawada T, Shishido T, Sugimachi M. Both skeletonized and pedicled internal thoracic arteries supply adequate graft flow after coronary artery bypass grafting even during intense sympathoexcitation. J Physiol Sci 60: 407-413, 2010.

35. Yokokawa M, Chugh A, Ulfarsson M, Takaki H, Han L, Yoshida K, Sugimachi M, Morady F, Oral H. Augmented ST-segment elevation during recovery from exercise predicts cardiac events in patients with Brugada syndrome. J Am Coll Cardiol. 56: 1576-1584, 2010

36. Kandori A, Ogata K, Miyashita T, Takaki H, Kanzaki H, Hashimoto S, Shimizu W, Kamakura S, Watanabe S, Aonuma K. Subtraction magnetocardiogram for detecting coronary heart disease. Ann Noninvasive Electrocardiol. 15: 360-368, 2010

37. Kawata H, Noda T, Kurita T, Yamagata K, Yamada Y, Okamura H, Satomi K, Shimizu W, Suyama K, Aihara N, Isobe M, Kamakura S. Clinical effect of implantable cardioverter defibrillator replacements: when should you resume driving after an implantable cardioverter defibrillator replacement? Circ J. 74: 2301-2307, 2010

38. Takigawa M, Noda T, Kurita T, Aihara N, Yamada Y, Okamura H, Satomi K, Suyama K, Shimizu W, Kamakura S. Predictors of electrical storm in patients with idiopathic dilated cardiomyopathy--how to stratify the risk of electrical storm. Circ J. 74: 1822-1829, 2010

39. Itoh H, Shimizu W, Hayashi K, Yamagata K, Sakaguchi T, Ohno S, Makiyama T, Akao M, Ai T, Noda T, Miyazaki A, Miyamoto Y, Yamagishi M, Kamakura S, Horie M. Long QT syndrome with compound mutations is associated with a more severe phenotype: a Japanese multicenter study. Heart Rhythm. 7: 1411-1418, 2010

40. Nagai T, Satomi K, Noda T, Okamura H, Yamada Y, Shimizu W, Suyama K, Aihara N, Kamakura S, Kurita T. Relationship between oral amiodarone and inappropriate therapy from an implantable cardioverter defibrillator. Circ J 74: 1302-1307, 2010

41. Matsuyama TA, Ishibashi-Ueda H, Ikeda Y, Yamada Y, Okamura H, Noda T, Satomi K, Suyama K, Shimizu W, Aihara N, Kamakura S, Inoue S. The positional relationship between the coronary sinus musculature and the atrioventricular septal junction. Europace. 12: 719-725, 2010

42. Watanabe H, Makiyama T, Koyama T, Kannankeril PJ, Seto S, Okamura K, Oda H, Itoh H, Okada M, Tanabe N, Yagihara N, Kamakura S, Horie M, Aizawa Y, Shimizu W. High prevalence of early repolarization in short QT syndrome. Heart Rhythm. 7: 647-652, 2010

43. Wu J, Shimizu W, Ding WG, Ohno S, Toyoda F, Itoh H, Zang WJ, Miyamoto Y, Kamakura S, Matsuura H, Nademanee K, Brugada J, Brugada P, Brugada R, Vatta M, Towbin JA, Antzelevitch C, Horie M. KCNE2 modulation of Kv4.3 current and its potential role in fatal rhythm disorders. Heart Rhythm 7: 199-205, 2010

44. Yokokawa M, Okamura H, Noda T, Satomi K, Suyama K, Kurita T, Aihara N, Kamakura S, Shimizu W. Neurally Mediated Syncope as a Cause of Syncope in Patients with Brugada Electrocardiogram. J Cardiovasc Electrophysiol. 21: 186-192, 2010

45. Seo K, Inagaki M, Nishimura S, Hidaka I, Sugimachi M, Hisada T, Sugiura S. Structural heterogeneity in the ventricular wall plays a significant role in the initiation of stretch-induced

arrhythmias in perfused rabbit right ventricular tissues and whole heart preparations. Circ Res. 106: 176-184, 2010

46. Okada J, Washio T, Hisada T. Study of efficient homogenization algorithms for nonlinear problems Approximation of a homogenized tangent stiffness to reduce computational cost. Comput Mech. 46: 247-258, 2010

47. Washio T, Okada J, Hisada T. A Parallel Multilevel Technique for Solving the Bidomain Equation on a Human Heart with Purkinje Fibers and a Torso Model. SIAM Review. 52: 717-743, 2010

48. 平林智子、岡田純一、鷲尾巧、杉浦清了、久田俊明; 力学・電気化学効果を考慮した心筋細胞モデル化に関する検討　日本機械学会論文集A 76: 1806-1815, 2010

49. 阿部誠、テルマ ケイコ スガイ、吉澤誠、山家智之、清水一夫、後藤萌、稲垣正司、杉町勝、砂川賢二；重回帰分析を用いた致死性不整脈検出アルゴリズムに関する検討　生体医工学　48: 577-583, 2010

Review

Am J Physiol Regul Integr Comp Physiol 300: R818–R826, 2011.
First published February 2, 2011; doi:10.1152/ajpregu.00426.2010.

Imbalance of central nitric oxide and reactive oxygen species in the regulation of sympathetic activity and neural mechanisms of hypertension

Yoshitaka Hirooka, Takuya Kishi, Koji Sakai, Akira Takeshita,† and Kenji Sunagawa

Department of Cardiovascular Medicine, Kyushu University Graduate School of Medical Sciences, Fukuoka, Japan

Submitted 29 June 2010; accepted in final form 29 January 2011

Hirooka Y, Kishi T, Sakai K, Takeshita A, Sunagawa K. Imbalance of central nitric oxide and reactive oxygen species in the regulation of sympathetic activity and neural mechanisms of hypertension. *Am J Physiol Regul Integr Comp Physiol* 300: R818–R826, 2011. First published February 2, 2011; doi:10.1152/ajpregu.00426.2010.— Nitric oxide (NO) and reactive oxygen species (ROS) play important roles in blood pressure regulation via the modulation of the autonomic nervous system, particularly in the central nervous system (CNS). In general, accumulating evidence suggests that NO inhibits, but ROS activates, the sympathetic nervous system. NO and ROS, however, interact with each other. Our consecutive studies and those of others strongly indicate that an imbalance between NO bioavailability and ROS generation in the CNS, including the brain stem, activates the sympathetic nervous system, and this mechanism is involved in the pathogenesis of neurogenic aspects of hypertension. In this review, we focus on the role of NO and ROS in the regulation of the sympathetic nervous system within the brain stem and subsequent cardiovascular control. Multiple mechanisms are proposed, including modulation of neurotransmitter release, inhibition of receptors, and alterations of intracellular signaling pathways. Together, the evidence indicates that an imbalance of NO and ROS in the CNS plays a pivotal role in the pathogenesis of hypertension.

blood pressure; sympathetic nervous system; central nervous system; nitric oxide; oxidative stress

ACTIVATION OF THE SYMPATHETIC nervous system is critically involved in the pathogenesis of hypertension, from initial occurrence to the development of target organ damage, such as heart failure, stroke, and renal failure (35, 36). The importance of the effects of the renin-angiotensin system on the sympathetic nervous system in the pathogenesis of hypertension is recently highlighted (30, 31). This is not surprising because both the autonomic nervous system and hormonal factors are the major regulators of blood pressure; therefore, abnormalities of either system are likely to be involved in the pathogenesis of essential hypertension (30, 31, 37). Esler (30) reported that the sympathetic nervous system is activated in ~50% of patients with hypertension, particularly in patients with essential hypertension. Central sympathetic outflow is determined by several important nuclei and their circuits in the central nervous system (CNS) (9, 81). These pathways involve many neurotransmitters and neuromodulators (16, 25, 38, 99). In particular, the brain stem circuitry is now considered crucial for the pathogenesis of hypertension, including both excitatory and inhibitory inputs from the supramedullary nuclei and the baroreceptors (16, 25, 38, 100, 115). In this review, we focus on the role of nitric oxide (NO) and reactive oxygen species (ROS) in the brain stem as factors constituting the neural mechanisms of hypertension. Because of the close relationship between NO and ROS, we discuss the individual roles of NO and ROS in the brain stem in central mechanisms of hypertension, and then the relationship between the two. Finally, we will discuss the possibility of targeting some cardiovascular drugs to improve the imbalance of NO and ROS.

NO in the Brain

NO is an important mediator of intracellular signaling in various tissues, including the CNS (32, 118, 119). NO acts via the second messenger cyclic GMP (32). Thus, soluble guanylate cyclase is its receptor. NO is synthesized from its precursor, L-arginine, by endogenous NO synthase (NOS). There are three NOS isoforms: constitutive enzymes, such as neuronal NOS (nNOS) and endothelial NOS (eNOS), and inducible enzymes such as inducible NOS (iNOS). A number of studies have demonstrated the localization of the nNOS, eNOS, and iNOS within the CNS using in situ hybridization and histochemical staining with NADPH-diaphorase or immunohistochemistry (8). nNOS is abundant in neurons. Considerable evidence indicates that NOS acts on central and peripheral sites throughout the autonomic nervous system, which controls the cardiovascular system, including the receptors and effectors of the baroreflex pathway (70, 95, 129).

Role of NO in the Brain Stem in Controlling Blood Pressure

Chronic administration of the NO synthesis inhibitor N^{ω}-nitro-L-arginine methyl ester (L-NAME) in drinking water induces a large increase in blood pressure in rats (29). Gangli-

† Deceased March 15, 2009.

Address for reprint requests and other correspondence: Y. Hirooka, Dept. of Cardiovascular Medicine, Kyushu Univ., Graduate School of Medical Sciences, 3-1-1 Maidashi, Higashi-ku, Fukuoka 812-8582, Japan (e-mail: hyoshi@cardiol.med.kyushu-u.ac.jp).

onic blockade elicits a greater fall in blood pressure in L-NAME-treated rats compared with controls, suggesting that the level of central sympathetic outflow in L-NAME-treated rats is greater than that in control rats. Microinjection of an ANG II type 1 (AT_1) receptor blocker (candesartan), but not that of an AT_2 receptor blocker (PD123319), into the nucleus tractus solitarius (NTS) elicits a greater decrease in blood pressure, heart rate, and renal sympathetic nerve activity (RSNA) in L-NAME-treated rats than in control rats. These results suggest that increased RSNA contributes to hypertension induced by chronic NOS inhibition and that activation of the renin-angiotensin system in the NTS is involved, at least in part, in the increased RSNA via AT_1 receptors (29). The rostral ventrolateral medulla (RVLM), the vasomotor center, is also activated in this model of hypertension, suggesting enhanced central sympathetic outflow (9). Pharmacological inhibition of NOS evoked by N^G-monomethyl-L-arginine (L-NMMA) or L-NAME also induces large increases in blood pressure that are partially sympathetically mediated in humans (109).

Immunohistochemical studies have revealed a rich distribution of nNOS in the NTS (8). Microinjection of L-NMMA into the NTS elicits an increase in blood pressure and RSNA, regardless of whether the baroreceptors are intact in anesthetized rabbits (39). The neurons in the NTS are activated by NO projecting to the caudal ventrolateral medulla, thereby activating the inhibitory neurons in the caudal ventrolateral medulla, which project to the RVLM, and may ultimately result in decreased sympathetic nerve activity (SNA). Single-unit extracellular recordings of NTS neurons in rat brain stem slices revealed that L-arginine increases neuronal activity dose-dependently, but D-arginine does not (80, 116). L-NMMA blocks the L-arginine-induced increases in the neuronal activity. Sodium nitroprusside, an NO donor, also increases neuronal activity. Consistent with the findings from the in vivo studies (39), these results suggest that NO increases the neuronal activity in the NTS through an increase in cyclic GMP. It has been proposed that NO acts in an ultrashort feedback loop, in which the release of L-glutamate activates nNOS and subsequently the production of NO (32). The NO, in turn, diffuses to presynaptic terminals, where it modulates the release of L-glutamate in response to neuronal activation. Studies using in vivo microdialysis demonstrated that activation of NMDA receptors in the NTS induces the release of NO, and NMDA-induced NO production stimulates L-glutamate release (74, 75, 82). In addition, this mechanism is involved in the depressor and bradycardic responses evoked by NMDA receptor activation in anesthetized rats (82). To determine the effects of increased NO production in the NTS for much longer periods on blood pressure, heart rate, and urinary norepinephrine excretion, we developed an in vivo technique for eNOS gene transfer into the NTS of rats (43, 44, 46, 107). In this study, the successful transfer of the eNOS gene into the NTS was confirmed by several methods, including immunohistochemistry, Western blot analysis, and nitrite/nitrate concentration measurements (107). Changes in blood pressure and heart rate were observed using a radio-telemetry system. It is important to note that we used eNOS instead of nNOS, which is normally abundant in the CNS, because the purpose of the study was to increase NO production from constitutively expressed NOS. The results indicated that NO in the NTS exerts an inhibitory effect on SNA in vivo.

Compared to studies of the NTS, studies of the RVLM in both acute and anesthestized models have produced more conflicting results (42, 53, 66, 81, 112, 120, 131). Therefore, we applied the technique described above to studies of the RVLM (57, 58). In those studies, blood pressure, heart rate, and urinary norepinephrine excretion were decreased after eNOS gene transfer. Microinjection of either L-NMMA or bicuculine, a GABA receptor antagonist, into the RVLM after eNOS gene transfer increased blood pressure to greater levels in the eNOS gene transfer group compared with the mock gene transfer control group. GABA levels in the RVLM after the eNOS gene transfer measured by in vivo microdialysis were also increased in the eNOS gene transfer group. These results indicate that the increased NO production evoked by the overexpression of eNOS in the bilateral RVLM decreases blood pressure, heart rate, and SNA in awake rats. Furthermore, these responses are mediated by an increased release of GABA in the RVLM. These studies provided convincing evidence that chronic changes in neurotransmitters/neuromodulators in the RVLM have a sustained impact on blood pressure in awake animals.

There is no clear explanation for the different modulatory effects of NO on neurons between the NTS and RVLM. NO increases both excitatory and inhibitory amino acids in the RVLM (43, 57). NO has also been shown to increase both L-glutamate and GABA in the paraventricular nucleus of hypothalamus (49). Microinjection of kynurenic acid into the RVLM, however, did not alter blood pressure after eNOS gene transfer, although microinjection of bicuculline into the RVLM augmented the increase in blood pressure (57). Therefore, we consider that GABAergic inhibition of the RVLM neurons might be more powerful than the glutamatergic activation in the resting condition (43, 57). In contrast, the glutamatergic input into the NTS neurons might be more powerful than the GABAergic input. In the NTS, there are close anatomic connections between nNOS and glutamatergic receptors (75). Furthermore, increases in NO induce L-glutamate release and microinfusion of NMDA and AMPA increase NO levels, suggesting that there are facilitatory interactions between L-glutamate and NO (27, 74, 82), although there are no studies measuring GABA levels induced by NO in the NTS. Furthermore, higher concentrations of NO are required to directly engage GABAergic inhibition, while lower concentrations of NO might be important for glutamatergic transmission in the NTS (125). Thus, it is still difficult and complicated to explain the physiological response induced by NO in the NTS (119). With regard to the action of NO on neuronal activity, NO induces both excitatory and inhibitory postsynaptic currents that likely depend on the neuron examined (6, 7, 126, 127).

Effects of NO in the Brain System in Experimental Models of Hypertension

Neurogenic mechanisms are dominant in the pathogenesis of essential hypertension in ~50% of patients (30). Spontaneously hypertensive rats (SHR) or stroke-prone SHR (SHRSP) exhibit increased RSNA during the development of hypertension, and blood pressure and RSNA are positively correlated (52, 79). The L-arginine-NO pathway is disrupted in SHR and SHRSP. The depressor response to an intracerebroventricular injection of an NO donor is greater in SHRSP than in normo-

tensive control rats, whereas the pressor response to intracerebroventricular injection of L-NAME is smaller (13). Semiquantitative RT-PCRs and in situ hybridization in SHR and Wistar-Kyoto (WKY) rats at 4 (prehypertensive) and 14 (established hypertension) wk of age (101) indicate that eNOS mRNA expression changes with the development of hypertension. Although there are no differences between the groups at 4 wk of age, nNOS gene expression increases in the hypothalamus, dorsal medulla, and caudal ventrolateral medulla of SHR compared with WKY rats at 14 wk of age. In the RVLM, there are no differences between the groups. In the SHRSP, there are also no differences in nNOS expression levels in the RVLM compared with WKY rats (101). A recent study demonstrated that NOS activity, measured by the ability of tissue homogenate to convert [^{3}H]L-arginine to [^{3}H]L-citrulline in a calcium- and NADPH-dependent manner, is impaired in the cerebral cortex and brain stem of prehypertensive SHR (104). In contrast, NOS activity is increased in the hypothalamus and brain stem in SHR rats with established hypertension compared with WKY rats (104). Thus, attenuated NOS activity in the cortex and brain stem of prehypertensive SHR might play a role in the pathogenesis of hypertension, and the up-regulated NOS activity in the hypothalamus and brain stem of SHR with established hypertension might serve to compensate for the hypertension. The expression of iNOS mRNA and protein is under the limits of detection in the hypothalamus of both WKY rats and SHR (40). Decreased NOS activity measured by the nitrite and nitrate contents was also demonstrated in the hypothalamus of SHR (1). In hypertensive SHRSP, nNOS protein expression levels in the hypothalamus and brain stem were enhanced compared with those in WKY (59). In a renovascular hypertensive rat model, mRNA expression levels of nNOS and soluble guanylate cyclase genes are reduced in the hypothalamus but not in the dorsal medulla (69). Together, these results suggest that the L-arginine-NO pathway is impaired in hypertensive rats, including SHR, possibly because of a posttranscriptional abnormality (70). Overexpression of eNOS in the NTS results in a greater depressor response in SHR than in WKY rats in the awake state (44). In that study, eNOS was used instead of nNOS to increase NO production locally in the NTS. Findings from another study suggest that the depressed NO modulation is consistent with the lower NOS activity in the dorsal brain stem (103). Therefore, the abnormality in the L-arginine-NO pathway in the NTS might be involved in the maintenance of hypertension of SHR. A recent study by Waki et al. (121) demonstrated that endogenous eNOS activity in the NTS plays a major role in determining the blood pressure set point in SHR and contributes to maintaining high arterial blood pressure in this model, suggesting the possible involvement of neurovascular coupling (96). In the RVLM of SHRSP, overexpression of eNOS elicits greater depressor and sympathoinhibitory responses than in WKY (58). Furthermore, the increase in NO production evoked by the overexpression of eNOS in the RVLM enhances the inhibitory action of GABA on the RVLM neurons (58). The results indicate that NO dysfunction and the resulting disinhibition of the RVLM contribute to increase RSNA in SHRSP.

Effects of NO in the Brain Stem on Baroreflex Function

As described earlier, NO activity in the NTS and RVLM influences cardiovascular regulation. We examined the role of endogenous NO in the brain stem in the rapid central adaptation of baroreflex control of RSNA in anesthetized rabbits (41). Bilateral carotid sinuses were isolated, and a stepwise increase in pressure was applied to the carotid sinuses, while arterial pressure and RSNA were recorded. The procedure was performed after intracisternal injection of L-NAME, D-NAME, L-arginine, or the vehicle solution. L-NAME enhances the rapid adaptation of the arterial baroreflex control of renal sympathetic nerve activity in rabbits (41). Transmission of arterial baroreflex signals depends on NO (27, 118). It was reported that the baroreceptor reflex gain in awake animals was increased by NO in the bradycardic component, although in these studies NOS inhibitors were administered systemically to examine the role of NO on baroreflex function (78, 87). Furthermore, overexpression of eNOS in the RVLM improves impaired baroreflex control of heart rate in SHRSP (60).

In summary, NO in the brain stem, particularly in the NTS and RVLM, has a sympathoinhibitory function, thereby reducing blood pressure. NO in the brain stem also facilitates the baroreflex function. The sympathoinhibitory effects of NO are impaired in animal models of hypertension, and supplementation of NO in the brain stem in hypertensive rats attenuates the abnormality, thereby decreasing blood pressure. The facilitory release of neurotransmitters induced by NO might be involved in the synaptic transmission mechanism.

ROS in the Brain

Substantial evidence also indicates that increased oxidative stress is involved in the pathogenesis of hypertension (12, 47, 48, 94, 99). ROS, such as superoxide anions and hydroxyl radicals, increase oxidative stress. There are several sources of ROS generation, such as NADPH oxidase, xanthine oxidase, mitochondria, and NOS uncoupling (12, 47, 48, 94, 99). On the other hand, reduction of antioxidant enzymes, such as superoxide dismutases (SOD), also induces an increase in oxidative stress (47, 48, 99). Although the role of ROS in the regulation of blood pressure in the normotensive state is not clear, increased ROS generation in the brain stem contributes to neural mechanisms of hypertension (47, 48). For example, although there is evidence of an increase in oxidative stress in the vasculature in hypertension, we showed, for the first time, that increased ROS in the RVLM contributes to SNA, leading to the neural mechanisms of hypertension in SHRSP (61). Zimmerman et al. (133) demonstrated that hypertension caused by low doses of circulating ANG II depends on the production of superoxide in the circumventricular organs (133). It was demonstrated that physiological responses to brain ANG II involve ROS production (15, 132, 133). Considering the importance of the brain ANG II system (2, 10, 26, 28, 83, 85, 86, 108), ROS play an important role in the neural regulation of blood pressure because ROS production largely depends on AT_1 receptor stimulation (47, 48, 99).

Role of ROS in Neural Mechanisms of Hypertension

As described earlier, on the basis of results demonstrating that microinjection of Tempol or overexpression of manga-

nese-superoxide dismutase in the RVLM markedly decreases blood pressure in SHRSP, but not in WKY, increased oxidative stress in the RVLM contributes to the neural mechanisms of hypertension in SHRSP (61). Oxidative stress levels in the RVLM were determined by measuring thiobarbituric acid-reactive substances (TBARS) levels and electron spin resonance (ESR) spectroscopy with a spin trapping technique (47, 48, 61). In SHR, oxidative stress in the RVLM plays an important role in hypertension via activation of the sympathetic nervous system (19, 66, 106, 117). An increase in oxidative stress in the RVLM also contributes to hypertension via activation of the sympathetic nervous system in rats with renovascular hypertension (two-kidney one-clip hypertensive model) (92). This model is an ANG II-dependent model of hypertension. Therefore, it is conceivable that ANG II increases oxidative stress by acting both centrally and peripherally, thereby activating the sympathetic nervous system and leading to hypertension as one of the hypertensive mechanisms in this model. AT_1 receptor expression levels in the RVLM and the paraventricular nucleus of the hypothalamus are enhanced in this rat renovascular model of hypertension (93). Interestingly, NADPH oxidase activity is increased, but Cu/Zn-SOD expression in the RVLM is unchanged. In a subsequent study, the authors showed that oxidative stress increased in both the RVLM and paraventricular nucleus, as well as systemically in this hypertensive model (93). These results suggest that systemic activation of the renin-angiotensin system activates AT_1 receptors in the brain, including the RVLM and paraventricular nucleus, thereby increasing SNA, leading to hypertension, as one of the mechanisms.

Sources of ROS Generation in the Brain Stem

NADPH oxidase is a major source of ROS in hypertension (71, 72) and has a critical role in generating ROS in the brain (5, 14, 51, 90, 122, 134). ANG II is upstream of NADPH oxidase activation, which requires Rac1 (48, 90, 122, 134). NADPH oxidase-derived ROS are involved in the effects of ANG II on Ca^{2+} influx in the NTS neurons receiving vagal afferents (122). Importantly, the essential subunit of NADPH oxidase, gp91phox, is present in somatodendritic and axonal profiles containing AT_1 receptors (122). The potentiation of Ca^{2+} currents indicates that ANG II increases neuronal excitability and spontaneous activity in some neurons (135). ANG II failed to increase ROS production or to potentiate L-type Ca^{2+} currents in the dorsomedial portion of the NTS neurons of mice lacking Nox2 (123). Thus, the excitatory actions of ANG II in the NTS neurons are caused, at least, in part, by the activation of L-type Ca^{2+} channels. It should be noted that ANG II-induced inhibition of neuronal delayed rectifying potassium current (I_{KV}) is mediated by ROS in primary neurons isolated from the hypothalamus and brain stem, because both NAD(P)H oxidase inhibition and Tempol prevented the ANG II inhibition of I_{KV} (113).

Mitochondria are another source of ROS generation in the brain. Chan et al. (21) examined the role of the mitochondrial electron transport chain in the RVLM of SHR and found that mitochondrial electron transport chain dysfunction in the RVLM of SHR depressed complex I or III activity and reduced the electron transport capacity (ETC) between complexes I and III or II and III (21). Interestingly, microinjection of coenzyme Q_{10} into the RVLM of SHR reversed the depressed ETC activity and enhanced superoxide generation. In addition, microinjection of antisense oligonucleotide against the p22phox subunit of NADPH oxidase into the RVLM reduced the enhanced ROS production in SHR (21). It is also important to note that microinjection of coenzyme Q_{10} into the RVLM of SHR decreases blood pressure (21). These results suggest that impairment of mitochondrial ETC complexes contributes to chronic oxidative stress in the RVLM of SHR, leading to enhanced central sympathetic drive and hypertension (21, 136). Consistent with their observation, we also found that ANG II induced the mitochondria-derived ROS production via activation of NADPH oxidase, although we did not find differences in the mitochondrial respiratory complexes between SHRSP and WKY (91), thus suggesting a feedforward system for ROS generation (21, 91, 136) (Fig. 1). Mitochondrial produced superoxide mediates the ANG II inhibition of I_{KV} (128). Recently, Chan et al. (22) suggested that transcriptional upregulation of mitochondrial uncoupling protein 2 (UCP2) in response to an increase in superoxide plays an active role in the feedback regulation of ROS production in the RVLM (22). Furthermore, oral treatment with rosiglitazone enhances a central antihypertensive effect via an upregulation of peroxisome proliferator-activated receptor-γ (PPAR-γ) and reduced oxidative stress in the RVLM of SHR (23). Stimulation of PPAR-γ results in the upregulation of UCP2, thereby reducing oxidative stress. The dose of rosiglitazone used in that study,

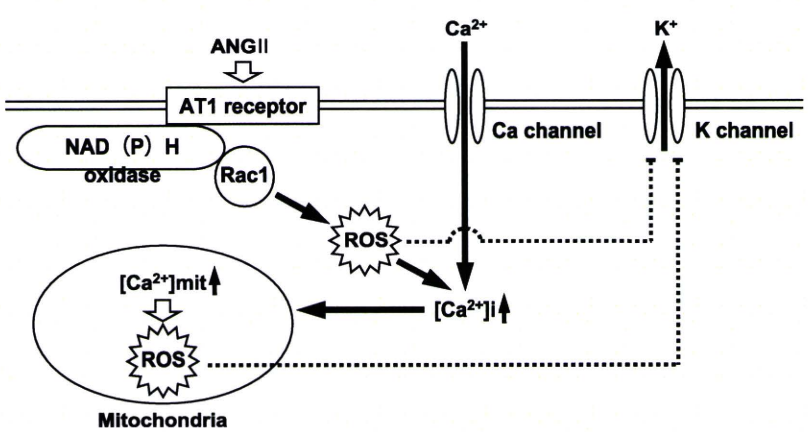

Fig. 1. A suggested scheme demonstrating that ANG II stimulation increases reactive oxygen species (ROS) generation via NAD(P)H oxidase and related mechanisms. [Modified from Nozoe et al. (91).]

however, was fairly high, and this does not necessarily relate to the clinical setting.

Downstream Signaling Pathway of the AT_1 Receptor Stimulation in the RVLM Involving ROS Production

As described above, activation of the AT_1 receptor produces superoxide anions as an initial step of ROS generation through NADPH oxidase. Thus, the signaling pathway should be pivotal for neuronal activation leading to hypertension via central sympathetic outflow. NAD(P)H oxidase-derived ROS production mediates the ANG II-induced pressor response via activation of p38 MAPK and ERK in the RVLM (18, 20). Chan et al. (20) demonstrated that intracerebroventricular infusion of ANG II elicits the long-term pressor response, and this pressor response is mediated by protein kinase C/ERK/cyclic adenosine monophosphate response element binding protein and c-*fos* induction (20). It should be noted that the ANG II-induced pressor response might not necessarily be related to ROS production in the RVLM. The ANG II-induced pressor response, however, is significantly inhibited by ROS scavenging, and endogenous blockade of AT_1 receptors in the brain stem of SHRSP reduces ROS and blood pressure (48, 91). Activation of caspase-3 acting through the Ras/p38 MAPK/ERK pathway in the RVLM might be involved in sympathoexcitation of SHRSP (65). In addition, the apoptotic proteins Bax and Bad are activated, and the antiapoptotic protein Bcl-2 is inhibited in the RVLM of SHRSP (65). The Ras inhibitor substantially attenuated these changes, thereby attenuating caspase-3 associated with the decrease in blood pressure. In contrast, however, c-Jun N-terminal kinase activity was not altered in the RVLM of SHRSP compared with that of WKY (65). It should be noted that the possibility of caspase-3-independent neuronal apoptosis in the RVLM or of a direct link between ROS and caspase-3 activation was not examined in that study (65). However, this finding is consistent with the results demonstrating that microinjection of ANG II induces AT_1 receptor-dependent ROS production and phosphorylation of p38 MAPK and ERK, but not stress-activated protein kinase/Jun N-terminal kinase in the RVLM of Sprague-Dawley rats (18). Interestingly, this is not the case in the RVLM of heart failure rabbits (77). Stress-activated protein kinase/Jun N-terminal kinase activity was increased in the RVLM of these heart failure rabbits (77). The increased phosphorylation of Jun N-terminal kinase may lead to activation of the transcription factor AP-1, which is a dimer of Jun and c-Fos family members. It is not clear why these differences between hypertension and heart failure occur. It is possible that signal transduction changes in the progression from hypertension to heart failure, thereby leading to further enhanced central sympathetic outflow. Further studies are needed to establish a more direct link between these signaling pathways, redox sensitivity, and the development and/or progression of hypertension.

Imbalance of Brain NO and ROS

Superoxide derived from NADPH oxidase reacts with and inactivates NO and thereby modulates its bioavailability (32, 97, 114) (Fig. 2). The converse is also true; that is, NO reduces superoxide, which may be beneficial (32, 99) (Fig. 2). An increase in NO in the RVLM decreases blood pressure and sympathetic nervous system activity to a greater extent in

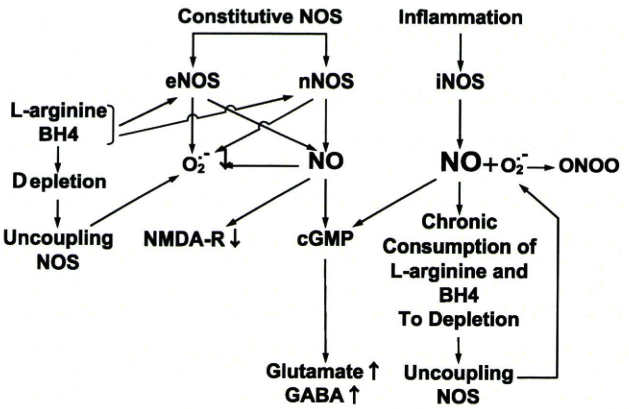

Fig. 2. A scheme demonstrating the interaction between nitric oxide (NO) and ROS generation. NMDA-R, *N*-methyl-D-aspartate receptors; GABA, γ-aminobutyric acid; BH4, tetrahydrobiopterin; NOS, nitric oxide synthase; eNOS, endothelial NOS; iNOS, inducible NOS; nNOS, neuronal NOS. [Modified from Hirooka (47).]

SHRSP than in WKY rats (58). This might be due to a reduction in superoxide via NO in the RVLM of SHRSP, which is increased in the RVLM of SHRSP (61). All three NOS isoforms generate superoxide depending on substrate (L-arginine) and cofactor (tetrahydrobiopterin) availability (32, 97, 114). The induction of both iNOS and ROS during inflammation is well established (88, 97). A recent study suggested that ROS and reactive nitrogen species, such as peroxynitrite dose-dependently regulate iNOS function (114). Overexpression of iNOS in the RVLM causes sympathoexcitation via an increase in oxidative stress (54). As expected, the release of more nitrite/nitrate (NO_x) in RVLM dialysate is induced by iNOS overexpression than by eNOS overexpression (54). Relative to the constitutive isoforms, iNOS has approximately five-fold higher NO production (97). NO_x release, however, is increased by approximately twofold higher by iNOS overexpression than by eNOS overexpression (54). We considered that the precursor of NO production, L-arginine, and its cofactor, tetrahydrobiopterin, might be consumed and insufficient when iNOS is chronically expressed, thereby iNOS would produce superoxide instead of NO (Fig. 2). Otherwise, chronic overexpression of iNOS increases levels of NO chronically, which, in turn, reacts with superoxide in a diffusion-limited reaction to produce peroxinitrite (Fig. 2). In fact, we found an increase in the TBARS levels in the RVLM and the pressor response after overexpression of iNOS. The increased pressor response was, however, abolished by iNOS inhibitors or Tempol. Once ROS production is increased, ROS enhance superoxide production from iNOS, indicating that ROS promote iNOS uncoupling. Further, peroxynitrite, produced from the reaction between NO and superoxide, reduces both NO and superoxide generation, indicating that peroxynitrite causes iNOS dysfunction enzymatically. In our study, we detected some iNOS-positive cells with the antinitrotyrosine antibody (54). Furthermore, iNOS expression levels were increased in the RVLM of SHRSP compared with WKY (56). Kung et al. (68) suggested that mitochondrial respiratory enzyme complexes in the RVLM were cellular targets of NO and ROS interaction after eNOS gene transfer. This concept is problematic, however, in that they suggest that superoxide and per-

oxynitrite are produced after eNOS gene transfer into the RVLM (68). Another recent study suggested that NMDA receptor activation increases ROS production through NO and Nox2 (33). Further studies are needed to explore whether this mechanism functions via ubiquitous glutamatergic synaptic transmission in vivo.

Sympathoinhibitory Effects of Antihypertensive Drugs and Statins

NADPH oxidase, which is activated by AT_1 receptor stimulation, is a major source of ROS (11, 17, 113, 135). The specific brain nuclei that regulate SNA, such as the anteroventral third ventricle, paraventricular nucleus of the hypothalamus, NTS, and the RVLM, are rich in AT_1 receptors (2, 10, 26, 28, 83). AT_1 receptor expression levels are upregulated in the RVLM of hypertensive animal models compared with normotensive controls (105). Thus, it is possible that AT_1 receptor blockers reduce oxidative stress in the brain, as well as in the peripheral vasculature. It is also possible that AT_1 receptor blockers inhibit ROS production by blocking AT1 receptor-mediated intracellular signaling (11, 48, 50) and that this antioxidant action accounts for the absence of reflex-induced sympathoexcitation after treatment with AT_1 receptor blockers. We evaluated the effects of AT_1 receptor blockers, olmesartan and telmisartan, on brain oxidative stress in SHRSP (4, 48). Both AT_1 receptor blockers have antioxidant properties in the brain without stimulating reflex-mediated SNA in SHRSP. We used in vivo ESR spectroscopy to examine the effect of oral olmesartan on oxidative stress in the brain (4), because the in vivo ESR method is a powerful technique for evaluating oxidative stress (3, 110, 111). The effects of peripherally administered olmesartan or telmisartan on central sympathetic outflow have been demonstrated in other studies (34, 76). Are these antioxidant effects of olmesartan or telmisartan specific for each drug or the AT_1 receptor blocker class? Other angiotensin receptor blockers, such as losartan or candesartan, have similar sympatho-inhibitory effects in the CNS, although there are some differences among angiotensin receptor blockers (24, 89, 102, 124). The differences of the central effects of each angiotensin receptor blocker might depend on its lipophilicity, phamacokinetics, and the transporter system (24, 34, 48, 124). Furthermore, systemically administered candesartan reduces brain ANG II via downregulation of the brain renin-angiotensin system (98). This finding provides new mechanistic insight into the treatment of hypertension by the AT_1 receptor blockers (84). Unfortunately, however, these effects of AT_1 receptor blockers, that is, reduction of brain oxidative stress and sympatho-inhibitory effects, even when administered systemically, are usually ignored by researchers or clinicians, but should be considered as potential therapeutic candidates.

Considering the inhibitory effects of AT_1 receptor blockers on brain oxidative stress and sympathetic nervous system activity, it would be interesting to know whether other cardiovascular drugs have similar effects. We found that atorvastatin causes depressor and sympathoinhibitory effects with upregulation of NOS in SHRSP (59), which is consistent with the effects of statins on eNOS upregulation in the vasculature (55). Atorvastatin also reduces oxidative stress in the RVLM of SHRSP (62, 63, 64). With regard to the central sympathoinhibitory effects of calcium channel blockers, lipophilic dihydropyridine calcium channel blockers, such as nifedipine, nisoldipine, and amlodipine, readily cross the blood-brain barrier, thereby presumably blocking brain L-type Ca^{2+} channels leading to central sympathoinhibition (73). It is generally considered that an arterial baroreflex-mediated increase in sympathetic activity is responsible for the unfavorable effects of short- and strong-acting dihydropyridine calcium channel blockers; therefore, the intrinsic sympathoinhibitory effects of calcium channel blockers have been ignored. These findings together suggest that increased NOS activity and antioxidant effects in the brain stem might be involved in the central sympathoinhibitory effects of some calcium channel blockers (45, 55, 67). The precise mechanisms involved, however, remain unknown, and further studies are required.

Summary and Conclusions

In summary, accumulating evidence indicates that an imbalance of NO and ROS in the CNS, particularly in the brain stem, is crucially involved in hypertension via the activation of central sympathetic outflow. Upstream and downstream consequences of the precise mechanisms are discussed. Several questions remain, however, because the interactions between NO and ROS are complex. Further studies are required to gain a better understanding of the role of brain NO and ROS in autonomic cardiovascular regulation and potential therapeutic targets.

GRANTS

This series of studies was supported by the Grants-in Aid for Scientific Research from the Japan Society for Promotion of Science and, in part, by a Grant from Kimura Memorial Foundation Research.

DISCLOSURES

No conflicts of interest, financial or otherwise, are declared by the authors.

REFERENCES

1. **Alaghband-Zadeh J, Das I, Hanson MR, MacGregor CAL, de Wardener HE, Laycock JF.** Hypothalamic and plasma total nitrate/nitrite concentrations in spontaneously hypertensive rats. *Exp Physiol* 81: 881–883, 1996.
2. **Allen AM, O'Callaghan EL, Chen D, Bassi JK.** Central neural regulation of cardiovascular function by angiotensin: a focus on the rostral ventrolateral medulla. *Neuroendocrinology* 89: 361–369, 2009.
3. **Anzai K, Saito K, Takeshita K, Takahashi S, Miyazaki H, Shoji H, Lee MC, Masumizu T, Ozawa T.** Assessment of ESR-CT imaging by comparison with autoradiography for the distribution of a blood-brain-barrier permeable spin probe, MC-PROXYL, to rodent brain. *Magn Reson Imaging* 21: 765–772, 2003.
4. **Araki S, Hirooka Y, Kishi T, Yasukawa K, Utsumi H, Sunagawa K.** Olmesartan reduces oxidative stress in the brain of stroke-prone spontaneously hypertensive rats assessed by an in vivo ESR method. *Hypertens Res* 32: 1091–1096, 2009.
5. **Bai Y, Jabbari B, Ye S, Campese VM.** Regional expression of NAD(P)H oxidase and superoxide dismutase in the brain of rats with neurogenic hypertension. *Am J Nephrol* 29: 483–492, 2009.
6. **Bains JS, Ferguson AV.** Nitric oxide depolarizes type II paraventricular nucleus neurons in vitro. *Neuroscience* 79: 149–159, 1997.
7. **Bains JS, Ferguson AV.** Nitric oxide regulates NMDA-drived GABAergic inputs to type I neurons of the rat paraventricular nucleus. *J Physiol* 499: 733–746, 1997.
8. **Batten TFC, Atkinson L, Deuchars J.** Nitric oxide systems in the medulla oblongata and their involvement in autonomic control. In: *Functional Neuroanatomy of the Nitric Oxide System. Handbook of Chemical Neuroanatomy*, edited by Steinbusch HWM, De Vente J, Vincent SR, Amsterdam, The Netherlands: Elsevier, 177–213, 2000.

9. **Bergamaschi CT, Campos RR, Lopes OU.** Rostral ventrolateral medulla: a source of sympathetic activation in rats subjected to long-term treatment with L-NAME. *Hypertension* 34: 744–747, 1999.
10. **Bourassa EA, Sved AF, Speth RC.** Angiotensin modulation of rostral ventrolateral medulla (RVLM) in cardiovascular regulation. *Mol Cell Endocrinol* 302: 167–175, 2009.
11. **Brandes RP.** Vascular functions of NADPH oxidases. *Hypertension* 56: 17–21, 2010.
12. **Briones AM, Touyz RM.** Oxidative stress and hypertension: current concepts. *Curr Hypertens Rep* 12: 135–142, 2010.
13. **Cabrena CL, Bealer SL, Bohr DF.** Central depressor action of nitric oxide is deficient in genetic hypertension. *Am J Hypertens* 9: 237–241, 1996.
14. **Campese VM, Sindhu RK, Ye S, Bai Y, Vaziri ND, Jabbari B.** Regional expression of NO synthase, NAD(P)H oxidase and superoxide dismutase in the rat brain. *Brain Res* 1134: 27–32, 2007.
15. **Campese VM, Shaohua Y, Huiquin Z.** Oxidative stress mediates angiotensin II-dependent stimulation of sympathetic nerve activity. *Hypertension* 46: 533–539, 2005.
16. **Campos RR, Bergamaschi CT.** Neurotransmission alterations in central cardiovascular control in experimental hypertension. *Curr Hypertens Rev* 2: 193–198, 2006.
17. **Campos RR.** Oxidative stress in the brain and arterial hypertension. *Hypertens Res* 32: 1047–1048, 2009.
18. **Chan SHH, Hsu KS, Huang CC, Wang LL, Ou CC, Chan JYH.** NADPH oxidase-derived superoxide anion mediates angiotensin II-induced pressor effect via activation of p38 mitogen-activated protein kinase in the rostral ventrolateral medulla. *Circ Res* 97: 772–780, 2005.
19. **Chan SHH, Tai MH, Li CY, Chan JYH.** Reduction in molecular synthesis or enzyme activity of superoxide dismutase and catalase contributes to oxidative stress and neurogenic hypertension in spontaneously hypertensive rats. *Free Radic Biol Med* 40: 2028–2039, 2006.
20. **Chan SHH, Wang LL, Tseng HL, Chan JYH.** Upregulation of AT_1 receptor gene on activation of protein kinase Cβ/nicotinamide adenine dinucleotide diphosphate oxidase/ERK1/2/c-*fos* signaling cascade mediates long-term pressor effect of angiotensin II in rostral ventrolateral medulla. *J Hypertens* 25: 1845–1861, 2007.
21. **Chan SHH, Wu KLH, Chang AYW, Tai MH, Chan JYH.** Oxidative impairment of mitochondrial electron transport chain complexes in rostral ventrolateral medulla contributes to neurogenic hypertension. *Hypertension* 53: 217–227, 2009.
22. **Chan SHH, Wu CA, Wu KLH, Ho YH, Chang AYW, Chang JYH.** Transcriptional upregulation of mitochondrial uncoupling protein 2 protects against oxidative stress-associated neurogenic hypertension. *Circ Res* 105: 886–896, 2009.
23. **Chan SHH, Wu KLH, Kung PSS, Chan JYH.** Oral intake of rosiglitazone promotes a central antihypertensive effect via upregulation of peroxisome proliferator-activated receptor- and alleviation of oxidative stress in rostral ventrolateral medulla of spontaneously hypertensive rats. *Hypertension* 55: 1444–1453, 2010.
24. **Culman J, Blume A, Gohlke P, Unger T.** The renin-angiotensin system in the brain: possible therapeutic implications for AT_1-receptor blockers. *J Hum Hypertens* 16: S64–S70, 2002.
25. **Dampney RAL.** Functional organization of central pathways regulating the cardiovascular system. *Physiol Rev* 74: 323–364, 1994.
26. **Dampney RAL, Fontes MAP, Hirooka Y, Potts PD, Tagawa T.** Role of angiotensin II receptors in the regulation of vasomotor neurons in the rostral ventrolateral medulla. *Clin Exp Pharmacol Physiol* 29: 467–472, 2002.
27. **Dias AC, Vitela M, Colombari E, Mifflin SW.** Nitric oxide modulation of glutamatergic, baroreflex, and cardiopulmonary transmission in the nucleus of the solitary tract. *Am J Physiol Heart Circ Physiol* 288: H256–H262, 2005.
28. **Dupont AG, Brouwers S.** Brain angiotensin peptides regulate sympathetic tone and blood pressure. *J Hypertens* 28: 1599–1610, 2010.
29. **Eshima K, Hirooka Y, Shigematsu H, Matsuo I, Koike G, Sakai K, Takeshita A.** Angiotensin in the nucleus tractus solitarii contributes to neurogenic hypertension caused by chronic nitric oxide synthase inhibition. *Hypertension* 36: 259–263, 2000.
30. **Esler M.** Sympathetic nervous activation in essential hypertension: commonly neglected as a therapeutic target, usually ignored as a drug side effect. *Hypertension* 55: 1090–1091, 2010.
31. **Esler M.** The 2009 Carl Ludwig Lecture. Pathophysiology of the human sympathetic nervous system in cardiovascular diseases: the translation from mechanisms to medical management. *J Appl Physiol* 108: 227–237, 2010.
32. **Garthwaite J.** Concepts of neural nitric oxide-mediated transmission. *Eur J Neurosci* 27: 2783–2802, 2008.
33. **Girouard H, Wang G, Gallo EF, Anthrather J, Zhou P, Pickel VM, Iadecola C.** NMDA receptor activation increases free radical production through nitric oxide and Nox2. *J Neurosci* 29: 2545–2552, 2009.
34. **Gohlke P, Weiss S, Jansen A, Wienen W, Stangier J, Rascher W, Culman J, Unger T.** AT1 receptor antagonist telmisartan administered peripherally inhibits central responses to angiotensin II in conscious rats. *J Pharmacol Exp Ther* 298: 62–70, 2001.
35. **Grassi G.** Assessment of sympathetic cardiovascular drive in human hypertension: achievements and perspectives. *Hypertension* 54: 690–697, 2009.
36. **Grassi G.** Sympathetic neural activity in hypertension and related diseases. *Am J Hypertens* 23: 1052–1060, 2010.
37. **Grassi G, Seravalle G, Quarti-Trevano F.** The 'neurogenic hypothesis' in hypertension: current evidence. *Exp Physiol* 95: 581–586, 2010.
38. **Guyenet PG.** The sympathetic control of blood pressure. *Nat Rev Neurosci* 7: 335–346, 2006.
39. **Harada S, Tokunaga S, Momohara M, Masaki H, Tagawa T, Imaizumi T, Takeshita A.** Inhibition of nitric oxide formation in the nucleus tractus solitarius increases renal sympathetic nerve activity in rabbits. *Circ Res* 72: 511–516, 1993.
40. **Haüser W, Sassmann A, Qadri F, Jöhren O, Dominiak P.** Expression of nitric oxide synthase isoforms in hypothalamo-pitutary-adrenal axis during the development of spontaneously hypertension in rats. *Mol Brain Res* 138: 198–204, 2005.
41. **Hironaga K, Hirooka Y, Matsuo I, Shihara M, Tagawa T, Harasawa Y, Takeshita A.** Role of endogenous nitric oxide in the brain stem on the rapid adaptation of baroreflex. *Hypertension* 31: 27–31, 1998.
42. **Hirooka Y, Polson JW, Dampney RAL.** Pressor and sympathoexcitatory effects of nitric oxide in the rostral ventrolateral medulla. *J Hypertens* 14: 1317–1324, 1996.
43. **Hirooka Y, Kishi T, Sakai K, Shimokawa H, Takeshita A.** Effect of overproduction of nitric oxide in the brain stem on the cardiovascular response in conscious rats. *J Cardiovasc Pharmacol* 41 *Suppl* 1: S119–S126, 2003.
44. **Hirooka Y, Sakai K, Kishi T, Ito K, Shimokawa H, Takeshita A.** Enhanced depressor response to endothelial nitric oxide synthase gene transfer into the nucleus tractus solitarii of spontaneously hypertensive rats. *Hypertens Res* 26: 325–331, 2003.
45. **Hirooka Y, Kimura Y, Nozoe M, Sagara Y, Ito K, Sunagawa K.** Amlodipine-induced reduction of oxidative stress in the brain is associated with sympatho-inhibitory effects in stroke-prone spontaneously hypertensive rats. *Hypertens Res* 29: 49–56, 2006.
46. **Hirooka Y.** Localized gene transfer and its application for the study of central cardiovascular control. *Auton Neurosci* 126–127: 120–129, 2006.
47. **Hirooka Y.** Role of reactive oxygen species in brainstem in neural mechanisms of hypertension. *Auton Neurosci* 142: 20–24, 2008.
48. **Hirooka Y, Sagara Y, Kishi T, Sunagawa K.** Oxidative stress and central cardiovascular regulation: pathogenesis of hypertension and therapeutic aspects. *Circ J* 74: 827–835, 2010.
49. **Horn T, Smith PM, McLaughlin BE, Bauce L, Marks GS, Pittman QJ, Ferguson AV.** Nitric oxide actions in paraventricular nucleus: cardiovascular and neurochemical implications. *Am J Physiol Regul Integr Comp Physiol* 266: R306–R313, 1994.
50. **Inaba S, Iwai M, Furuno M, Tomono Y, Senba I, Okayama H, Mogi M, Higaki J, Horiuchi M.** Continuous activation of renin-angiotensin system impairs cognitive function in renin/angiotensinogen transgenic mice. *Hypertension* 53: 356–362, 2009.
51. **Infanger DW, Shrama RV, Davisson RL.** NADPH oxidases of the brain: distribution, regulation, and function. *Antioxid Redox Signal* 8: 1583–1596, 2006.
52. **Judy WV, Watanabe AM, Henry DP, Besch HR, Murphy WR, Hockel GM.** Sympathetic nerve activity: role in regulation of blood pressure in the spontaneously hypertensive rat. *Circ Res* 38: I-121–I-129, 1976.
53. **Kagiyama S, Tsuchihashi T, Abe I, Fujishima M.** Cardiovascular effects of nitric oxide in the rostral ventrolateral medulla of rats. *Brain Res* 757: 155–158, 1997.
54. **Kimura Y, Hirooka Y, Sagara Y, Ito K, Kishi T, Shimokawa H, Takeshita A, Sunagawa K.** Overexpression of inducible nitric oxide synthase in rostral ventrolateral medulla causes hypertension and sym-

pathoexcitation via an increase in oxidative stress. *Circ Res* 96: 252–260, 2005.

55. **Kimura Y, Hirooka Y, Sagara Y, Sunagawa K.** Long-acting calcium channel blocker, azelnidipine, increases endothelial nitric oxide synthase in the brain and inhibits sympathetic nerve activity. *Clin Exp Hypertens* 29: 13–21, 2007.
56. **Kimura Y, Hirooka Y, Kishi T, Ito K, Sagara Y, Sunagawa K.** Role of inducible nitric oxide synthase in rostral ventrolateral medulla in blood pressure regulation in spontaneously hypertensive rats. *Clin Exp Hypertens* 31: 281–286, 2009.
57. **Kishi T, Hirooka Y, Shigematsu H, Shimokawa H, Takeshita A.** Overexpression of eNOS in the RVLM causes hypotension and bradycardia via GABA release. *Hypertension* 38: 896–901, 2001.
58. **Kishi T, Hirooka Y, Ito K, Sakai K, Shimokawa H, Takeshita A.** Cardiovascular effects of overexpression of endothelial nitric oxide synthase in the rostral ventrolateral medulla in stroke-prone spontaneously hypertensive rats. *Hypertension* 39: 264–268, 2002.
59. **Kishi T, Hirooka Y, Mukai Y, Shimokawa H, Takeshita A.** Atorvastatin causes depressor and sympatho-inhibitory effect with upregulation of nitric oxide synthases in stroke-prone hypertensive rats. *J Hypertens* 21: 379–386, 2003.
60. **Kishi T, Hirooka Y, Kimura Y, Sakai K, Ito K, Shimokawa H, Takeshita A.** Overexpression of eNOS in RVLM improves impaired baroreflex control of heart rate in SHRSP. *Hypertension* 41: 255–260, 2003.
61. **Kishi T, Hirooka Y, Kimura Y, Ito K, Shimokawa H, Takeshita A.** Increased reactive oxygen species in rostral ventrolateral medulla contribute to neural mechanisms of hypertension in stroke-prone spontaneously hypertensive rats. *Circulation* 109: 2357–2362, 2004.
62. **Kishi T, Hirooka Y, Shimokawa H, Takeshita A, Sunagawa K.** Atorvastatin reduces oxidative stress in the rostral ventrolateral medulla of stroke-prone spontaneously hypertensive rats. *Clin Exp Hypertens* 30: 3–11, 2008.
63. **Kishi T, Hirooka Y, Konno S, Sunagawa K.** Atorvastatin improves the impaired baroreflex sensitivity via anti-oxidant effect in the rostral ventrolateral medulla of SHRSP. *Clin Exp Hypertens* 31: 698–704, 2009.
64. **Kishi T, Hirooka Y, Konno S, Sunagawa K.** Sympathoinhibition induced by centrally administered atorvastatin is associated with alteration of NAD(P)H and Mn-SOD activity in rostral ventrolateral medulla of stroke-prone SHR. *J Cardiovasc Pharmacol* 55: 184–190, 2010.
65. **Kishi T, Hirooka Y, Konno S, Ogawa K, Sunagawa K.** Angiotensin type 1 receptor-activated caspase-3 through ras/mitogen-activated protein kinase/extracellular signal-regulated kinase in the rostral ventrolateral medulla is involved in sympathoexcitation in stroke-prone spontaneously hypertensive rats. *Hypertension* 55: 291–297, 2010.
66. **Koga Y, Hirooka Y, Araki S, Nozoe M, Kishi T, Sunagawa K.** High salt intake enhances blood pressure increase during development of hypertension via oxidative stress in rostral ventrolateral medulla of spontaneously hypertensive rats. *Hypertens Res* 31: 2075–2083, 2008.
67. **Konno S, Hirooka Y, Araki S, Koga Y, Kishi T, Sunagawa K.** Azelnidipine decreases sympathetic nerve activity via antioxidant effect in the rostral ventrolateral medulla of stoke-prone spontaneously hypertensive rats. *J Cardiovasc Pharmacol* 52: 555–560, 2008.
68. **Kung LC, Chan SHH, Wu KLH, Ou CC, Tai MH, Chan JYH.** Mitochondrial respiratory enzyme complexes in rostral ventrolateral medulla as cellular targets of nitric oxide and superoxide interaction in the antagonism of antihypertensive action of eNOS transgene. *Mol Pharmacol* 74: 1319–1332, 2008.
69. **Kurukoff TL, Gehlen F, Ganten D, Wagner J.** Gene expression of brain nitric oxide synthase and soluble guanylate cyclase in hypothalamus and medulla of two-kidney, one-clip hypertensive rats. *Hypertension* 26: 171–176, 1995.
70. **Krukoff TL.** Central action of nitric oxide in regulation of autonomic functions. *Brain Res Rev* 30: 52–65, 1999.
71. **Lambeth JD.** Nox enzymes, ROS, and chronic disease: an example of antagonistic pleiotropy. *Free Radic Biol Med* 43: 332–347, 2007.
72. **Lassegue B, Clempus RE.** Vascular NAD(P)H oxidases: specific features, expression, and regulation. *Am J Physiol Regul Integr Comp Physiol* 285: R277–R297, 2003.
73. **Leenen FHH, Ruzicka M, Huang BS.** Central sympathoinhibitory effects of calcium channel blockers. *Curr Hypertens Res* 3: 314–321, 2001.
74. **Lin HC, Kang BH, Wan FJ, Huang ST, Tseng CJ.** Reciprocal regulation of nitric oxide and glutamate in the nucleus tractus solitarii of rats. *Eur J Pharmacol* 407: 83–89, 2000.
75. **Lin LH.** Glutamatergic neurons say NO in the nucleus tractus solitarii. *J Chem Neuroanat* 38: 1154–165, 2009.
76. **Lin Y, Matsumura K, Kagiyama S, Fukuhara M, Fujii K, Iida M.** Chronic administration of olmesartan attenuates the exaggerated pressor response to glutamate in the rostral ventrolateral medulla of SHR. *Brain Res* 1058: 161–166, 2005.
77. **Liu D, Gao L, Roy SK, Cornish KG, Zucker IH.** Neuronal angiotensin II type 1 receptor upregulation in heart failure: activation of activator protein 1 and jun N-terminal kinase. *Circ Res* 99: 1004–1011, 2006.
78. **Liu JL, Murakami H, Zucker IH.** Effects of NO on baroreflex control of heart rate and renal nerve activity in conscious rabbits. *Am J Physiol Regul Integr Comp Physiol* 270: R1361–R1370, 1996.
79. **Luft FC, Demmert G, Rohmeiss P, Unger T.** Baroreceptor reflex effect on sympathetic nerve activity in stroke-prone spontaneously hypertensive rats. *J Auton Nerv Syst* 17: 199–209, 1986.
80. **Ma S, Abboud FM, Felder RB.** Effects of L-arginine-derived nitric oxide synthesis on neuronal activity in nucleus tractus solitarius. *Am J Physiol Regul Integr Comp Physiol* 268: R487–R491, 1995.
81. **Marting-Pinge MC, Baraldi-Passy I, Lopes OU.** Excitatory effects of nitric oxide within the rostral ventrolateral medulla of freely moving rats. *Hypertension* 30: 704–707, 1997.
82. **Matsuo I, Hirooka Y, Hironaga K, Eshima K, Shigematsu H, Shihara M, Sakai K, Takeshita A.** Glutamate release via NO production evoked by NMDA in the NTS enhances hypotension and bradycardia in vivo. *Am J Physiol Regul Integr Comp Physiol* 280: R1285–R1291, 2001.
83. **McKinley MJ, Albinson AL, Allen AM, Mathai M, May CN, McAllen RM, Oldfield BJ, Mendelsohn FAO, Chai SY.** The brain renin-angiotensin system: location and physiological roles. *Int J Biochem Cell Biol* 35: 901–918, 2003.
84. **Mogi M, Horiuchi M.** Remote control of brain angiotensin II levels by angiotensin receptor blockers. *Hypertens Res* 33: 116–117, 2010.
85. **Morimoto S, Cassel MD, Beltz TG, Johnson AK, Davisson RL, Sigmund CD.** Elevated blood pressure in transgenic mice with brain-specific expression of human angiotensinogen driven by the glial fibrillary acidic protein promoter. *Circ Res* 89: 365–372, 2001.
86. **Morimoto S, Cassell MD, Sigmund CD.** The brain renin-angiotensin system in transgenic mice carrying a highly regulated human renin transgene. *Circ Res* 90: 80–86, 2002.
87. **Murakami H, Liu JL, Yoneyama H, Nishida Y, Okada K, Kosaka H, Morita H, Zucker IH.** Blockade of neuronal nitric oxide synthase alters the baroreflex control of heart rate in the rabbit. *Am J Physiol Regul Integr Comp Physiol* 274: R181–R186, 1998.
88. **Murphy S, Gibson CL.** Nitric oxide, ischaemia and brain inflammation. *Biochem Soc Trans* 35: 1133–1137, 2007.
89. **Nishimura Y, Ito T, Hoe KL, Saavedra JM.** Chronic peripheral administration of the angiotensin II AT_1 receptor antagonist candesartan blocks brain AT_1 receptors. *Brain Res* 871: 29–38, 2000.
90. **Nozoe M, Hirooka Y, Koga Y, Sagara Y, Kishi T, Engelhardt JF, Sunagawa K.** Inhibition of rac1-derived reactive oxygen species in nucleus tractus solitarius decreases blood pressure and heart rate in stroke-prone spontaneously hypertensive rats. *Hypertension* 50: 62–68, 2007.
91. **Nozoe M, Hirooka Y, Koga Y, Araki S, Konno S, Kishi T, Ide T, Sunagawa K.** Mitochondria-derived reactive oxygen species mediate sympathoexcitation induced by angiotensin II in the rostral ventrolateral medulla. *J Hypertens* 26: 2176–2184, 2008.
92. **Oliveira-Sales EB, Dugaich AP, Carillo BA, Abreu NP, Boim MA, Martins PJ, D'Almeida V, Dolnkoff MS, Bergamaschi CT, Campos RR.** Oxidative stress contributes to renovascular hypertension. *Am J Hypertens* 21: 98–104, 2008.
93. **Oliveira-Sales EB, Nishi EE, Carillo BA, Dolnikoff MS, Bergamaschi CT, Campos RR.** Oxidative stress in the sympathetic premotor neurons contributes to sympathetic activation in renovascular hypertension. *Am J Hypertens* 22: 484–492, 2009.
94. **Paravicini T, Touyz RM.** Redox signaling in hypertension. *Cardiovasc Res* 71: 247–258, 2006.
95. **Patel KP, Li YF, Hirooka Y.** Role of nitric oxide in central sympathetic outflow. *Exp Biol Med (Maywood)* 226: 814–824, 2001.